Received: 21 January 2021 | Revised: 1 March 2021 | Accepted: 10 March 2021

DOI: 10.1111/ijag.15919

INTERNATIONAL JOURNAL OF Applied Glass SCIENCE

SPECIAL ISSUE ARTICLE

Two-step ion-exchanged soda lime silicate glass: Effect of surface compression on silver ion release

Ali Talimian[1] | Aleksandra Nowicka[1] | Hana Kaňková[1] | Gohar Sani[2] | Dagmar Galusková[1] | Lothar Wondraczek[2] | Dusan Galusek[1,3]

[1]Centre for Functional and Surface Functionalised Glass, Alexander Dubcek University of Trencin, Trencin, Slovakia

[2]Otto Schott Institute of Materials Research, University of Jena, Jena, Germany

[3]Joint Glass Centre of the IIC SAS, TnUAD and FChPT STU, Trencin, Slovakia

Correspondence
Ali Talimian, Centre for Functional and Surface Functionalised Glass, Alexander Dubcek University of Trencin, Trencin, Slovakia.
Email: ali.talimian@tnuni.sk

Lothar Wondraczek, Otto Schott Institute of Materials Research, University of Jena, Jena, Germany.
Email: lothar.wondraczek@uni-jena.de

Funding information
Vedecká Grantová Agentúra MŠVVaŠ SR a SAV, Grant/Award Number: 1/0911/20 and 2/0028/21; H2020 Spreading Excellence and Widening Participation, Grant/Award Number: 739566

Abstract

Although glass plays an important role in medical facilities such as countertops or interfaces of medical equipment, where chemical and mechanical durability is of great concern, less attention has been paid to developing durable anti-microbial surfaces. In the present work, silver-containing surfaces were produced by ion exchange in soda-lime silicate float glass, and the effects of residual surface compression produced by ion-exchange on the release of silver ions were investigated. Silver-doped surfaces were prepared by a sequential two-stage ion-exchange process in pure potassium nitrate, at 450°C for 4-24 hours, and subsequently in KNO_3+ 1 wt% $AgNO_3$, at 400°C for 10-30 minutes. Silver ions were found to penetrate 3-5 μm into the glass surface, causing only a limited decrease in surface compression induced by potassium ions. The silver-rich layer provides the required Ag^+ leaching essential for anti-microbial applications, as confirmed by Ag^+ ion leaching tests. The silver release can be altered by surface compression.

KEYWORDS

ion release, ion-exchange, soda-lime silicate, strengthening

1 | INTRODUCTION

Glass, especially soda lime silicate glass (SLS), surfaces play an integral role in human life: we constantly interact with SLS and other silicate glass surfaces. A contact with glass surfaces represents an increased risk of infection spread from microbes residing on the glass surfaces; such risk spikes in case of hospital-associated infections.[1,2] Although the surfaces can be cleaned using chemicals, there are concerns about the exposure of health care personnel to the anti-microbial agents.[3-5] Self-disinfecting surfaces are an alternative solution to the use of disinfectants for reducing microbial activity; different strategies have been proposed for anti-bacterial applications: for instance, coating the glass surfaces with a layer containing active eluting agents such as silver, copper, tungsten or zinc nanoparticles, or introducing silver directly to the glass composition. [3,6-11] Most prominently, Ag^+ release from the glass surface is a practical method to prevent microbial activity[1,12,13]. While introducing silver to the glass composition significantly increases the production cost, covering the glass surface with silver-containing coatings, using, for example, sol-gel methods, is

economically favorable. However, the coatings' mechanical performance and durability are questionable.[14]

Ag^+-Na^+ ion-exchange is a well-established technique to modify the optical properties of soda lime silicate glass by replacing glass sodium ions with silver ions at the surface.[15-20] Moreover, if Na^+ ions are replaced with larger potassium ions at a temperature below the glass transition temperature, the "stuffing" effect produces surface compression that improves the practical strength.[21] When K^+-Na^+ ion-exchange is done in order to improve mechanical properties, it is also called chemical strengthening.[22-24] In typical industrial situations, chemical strengthening of SLS glass is performed by placing glass components for several hours in a molten potassium nitrate salt bath.[25] Although both Ag^+-Na^+ and K^+-Na^+ ion-exchange can be carried out simultaneously using a salt mixture of potassium nitrate and silver nitrate, large amounts of silver penetrate into the glass, deteriorating the efficiency of chemical strengthening with no beneficial impact on antibacterial activity.[26,27]

Multi-step ion-exchange can be used to produce different ion-exchanged layers on a glass surface.[28,29] The production of different layers with various chemical compositions can provide anti-microbial properties and, at the same time, improve mechanical performance. In this work, commercial soda-lime silicate float glass was subjected to a two-step ion-exchange to introduce silver to the glass surface and suppress the surface compression degradation so as to obtain glasses which are simultaneously strengthened and silver-releasing. The produced samples were then characterized in terms of silver and potassium concentration at their surface, residual stress, and silver release to define the silver release's influential factors.

2 | EXPERIMENTAL PROCEDURE

Soda-lime silicate float glass with a thickness of ca. 4 mm used in the present work was obtained from a commercial source (AGC Trencin, s.r.o., AGC Europa). The softening temperature of the glass, T_s, was determined using a thermomechanical analyzer, TMA, (TMA 402 Hyperion, Netzsch, Germany) following the ASTM C338-93 norm.[30] The glass softening temperature is at approximately 568 ± 2°C. The Na_2O and K_2O content in the used glass was measured by X-Ray Fluorescence method using a wavelength dispersive spectrometer (S8 TIGER 4 kW, Bruker, Billerica, MA, USA) equipped with an X-ray tube with Rh anode (30 kV and 100 mA). The glass contains 12.70 ± 0.50 mol% Na_2O and 0.10 ± 0.03 mol% K_2O.

Three different salt baths were used for ion-exchange processes: pure KNO_3, KNO_3 + 0.2 wt% $AgNO_3$, and KNO_3 + 1.0 wt% $AgNO_3$. Potassium nitrate (Sigma-Aldrich, ACS grade >99.0) and $AgNO_3$ (Sigma-Aldrich, ACS grade >99.0) were used to prepare the salt baths. The salts were dried at 105°C for 72 hours and mixed. The salt baths were prepared by melting the mixtures at 450°C for 8 hours. Square samples, nominally 30 × 30 mm, were cut from the original glass sheet. The sharp edges of samples were polished using 125 μm diamond grinding disks. The samples were ultrasonically cleaned in deionized water, washed with isopropyl alcohol, and dried at 70°C overnight.

Ion-exchange treatments were carried out in the molten salts using stainless steel crucibles kept in a laboratory muffle furnace; the glass-to-salt weight ratio was always kept below 1:20. Single-step ion-exchange processes were conducted at 450°C for 4 hours and 24 hours in KNO_3, KNO_3 + 0.2 wt% $AgNO_3$, and KNO_3 + 1.0 wt% $AgNO_3$. Two-step ion exchanges were performed on the samples subjected to ion-exchange at 450°C in pure potassium nitrate for 4 and 24 hours; then, the ion-exchanged samples were immersed in the potassium nitrate salt bath containing 1.0 wt% $AgNO_3$ at 400°C for 10 minutes and 30 minutes. Samples were kept at 350°C for 10 minutes before and after ion-exchange to avoid thermal shock.

Surface compression was measured using a surface stress meter (FSM 6000, Luceo Co Ltd., Tokyo, Japan) according to ASTM C1279-13 norm[31]; the measurements were performed only on the gas side of the glass; the surface compression was measured on at least five samples. The measurement was repeated twice for each sample, and the sample was rotated 90°C before the second measurement.

Vickers' indentation was carried out using a maximum load of 1 kgf and 15 seconds holding time; the indentations were produced in ambient air (T = 20°C and relative humidity 50%). At least 10 indentations were performed for each sample. The optical micrographs were taken using a wide-field confocal microscope (Zeiss Smartproof 5, Zeiss, Jena, Germany) a few seconds after indentation to avoid humidity-induced subcritical crack growth.

Ion-release experiments were carried out on the gas side of samples; the tin-side was covered using a temperature-resistant paint. Afterward, the samples were immersed in 10 ml of deionized water in a Teflon vessel and kept at 40°C for 24 hours. The amounts of ions leached from glass (Ag, Na, K, Fe, Ca, Mg, Al, and Si) to the corrosion solution were determined by Inductively Coupled Plasma Optical Emission Spectroscopy (ICP-OES Agilent 5100 SVDV, Agilent Technologies Inc., Santa Clara, CA). The calibration solutions for ICP analyses were prepared from single-element standards (Analytika, Prague, Czech Republic) with a concentration of 1000 ÷ 2 $mg \cdot l^{-1}$ of Ag, Na, K, Fe, Ca, Mg, Al, and Si. Along with the testing of the corrosion solutions, analyses of blank solutions (test corrosion medium without any sample) were carried out. The analyses of blank samples were conducted to exact the measured values of individual element concentrations relating to the content of the elements

present in the blank and not originating from prepared glass samples.

Transmission spectra were measured in the wavelength range between 200 and 2000 nm using a UV-Vis-NIR spectrophotometer (Cary 5000, Agilent, Santa Clara, CA).

The semi-quantitative concentration of specific elements (Si, K, Ca, Mg, Na, and Ag) was measured on a clean region of about 0.5 mm^2 on the gas side of samples by energy dispersion X-ray spectroscopy (Aztec EDX, Oxford Instruments, Oxford, UK) within SEM (JEOL 7600F, Tokyo, Japan); accelerating voltage of 15 kV and dwelling time of 15 seconds were used. The concentrations of sodium, potassium, and silver were calculated by assuming that the elements exist as Na_2O, K_2O, and Ag_2O in the glass. Before analysis, the samples were coated with Au-Pd alloy using SEM sputter coater (JEOL JFC-1300, Japan). The depth of the ion-exchanged layer, DOL, was measured at the fracture surface of ion-exchanged samples near the gas side on a straight line from the surface to a depth of about 50-200 μm; the noise of the microprobe analysis was reduced by the moving average method. The measurements were carried out over at least five different spots.

3 | RESULTS

Table 1 summarizes the residual surface compression produced by performing a single-step ion-exchange at 450°C for 4 and 24 hours in salt baths with different amounts of $AgNO_3$. Longer processes produced smaller surface compression and deeper compressive layers than the shorter ion-exchanges: Thee surface compressive stress is around 550-590 MPa for samples subjected to ion-exchange for 4 hours, whereas it is about 400-450 MPa for the sample ion-exchanged for 24 hours. These values compare-well to ion-exchange properties of similar SLS glasses.[32,33] The ion-exchange for 4 and 24 hours produced a compressive layer with a thickness of 11 and 27 μm, respectively. However, the thickness of the ion-exchanged layer was larger than the measurement window of the surface stress meter for samples subjected to ion-exchanged in KNO_3 + 1.0 wt% $AgNO_3$; measuring the surface compression was therefore not possible.

Figure 1 shows representative imprints produced by Vickers indentation on the as-received and ion-exchanged glass using 1 kgf load. Radial cracks are visible in the as-received glass, while no cracks are observed in the glass subjected to ion-exchange for 4 hours in KNO_3. This indicates that the surface compression is sufficient to prevent crack formation or extension. Conversely, the samples subjected to ion-exchange in $AgNO_3$ containing salts show cracks at the edges of indentation imprint. This indicates, in contrast with the stress measured by the surface stress meter, that the surface compression of samples ion-exchanged in silver-containing salts is smaller than the samples ion-exchanged in pure KNO_3. The overestimation of surface compression is the result of the changes in the refractive index of glass after silver penetration.[34] The ion-exchanged glass in KNO_3-1.0 wt% $AgNO_3$ exhibits larger cracks than that prepared in KNO_3-0.2 wt% $AgNO_3$. Moreover, the light birefringence patterns around the indentation indicate lateral cracks beneath the surface of samples ion-exchanged for 24 hours in pure KNO_3 and in the salt with 0.2 wt% $AgNO_3$. The ion-exchanged glass in KNO_3-1.0 wt% $AgNO_3$ exhibits mainly radial/median cracks.

Table 2 summarizes the surface compression in the samples subjected to a two-step ion-exchange. The produced surface compression by the first ion-exchange at 450°C in KNO_3 remains substantially unchanged after the second ion-exchange. However, it was impossible to measure the surface compression of samples prepared by performing the first ion-exchange for 4 hours and the second ion-exchange for 30 minutes. Figure 2 shows indentations produced on the gas side of samples subjected to two-step ion-exchange using the load of 1 kgf. Although small cracks are visible surrounding the indentations, they are smaller than those observed in the single-step ion-exchanged sample in KNO_3-1.0 wt% $AgNO_3$ for 24 hours. This indicates that although the second ion-exchange decreases the surface residual stress, it reduces the surface compression less than the long treatments in silver-containing salts.

Figure 3 shows the semi-quantitative molar concentrations of Na_2O, K_2O, and Ag_2O on the surface of treated samples; the surface composition of as-received glass is also shown for comparison. Although sodium is largely substituted with potassium by K^+-Na^+ ion-exchange, there

TABLE 1 Compressive surface residual stress and case depth (± SD) of samples produced by single-step ion-exchange (N.D.: not determined)

Salt composition	KNO_3		KNO_3 + 0.2 wt% $AgNO_3$		KNO_3 + 1.0 wt% $AgNO_3$	
Time (h)	4	24	4	24	4	24
Surface Compression (MPa)	566 ± 5	411 ± 26	587 ± 5	448 ± 5	N.D.	N.D.
Case depth (μm)	11 ± 1	27 ± 1	10 ± 1	27 ± 1	N.D.	N.D.

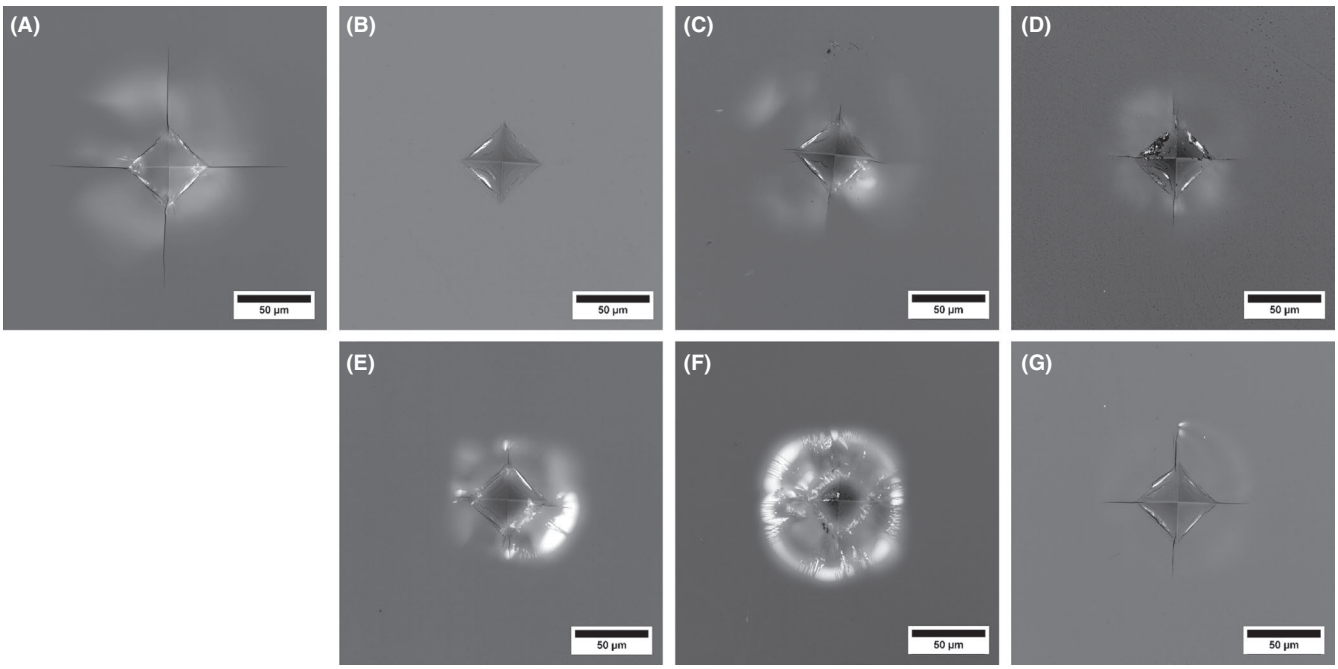

FIGURE 1 Indentations produced with 1 kgf on the gas side of (A) as-received glass, samples subjected to single-step ion-exchange for 4 h in (B) KNO_3, (C) KNO_3+ 0.2 wt% $AgNO_3$, (D) KNO_3+ 1.0 wt% $AgNO_3$, and for 24 h in (E) KNO_3, (F) KNO_3+ 0.2 wt% $AgNO_3$, (G) KNO_3+ 1.0 wt% $AgNO_3$

TABLE 2 Compressive surface residual stress and case depth (± SD) of samples produced by two-step ion-exchange (N.D.: not determined)

First Ion-exchange conditions	KNO_3-4 h		KNO_3-24 h	
Second ion-exchange time (min)	10	30	10	30
Surface Compression (MPa)	548 ± 3	N.D.	442 ± 7	450 ± 4

is still a limited amount of residual sodium present in the samples. The surface compositions of the samples ion-exchanged in pure KNO_3 for 4 hours, and 24 hours are similar. Moreover, the samples ion-exchanged in KNO_3-0.2 wt% $AgNO_3$ for 4 hours show a very similar surface composition as the samples treated in pure KNO_3; however, the concentration of K_2O increases slightly in samples subjected to 24 hours ion-exchange, with some traces of Ag_2O on the surface. It is important to mention that a relatively large error accompanies the reported silver concentrations; it is perceivable that the reported Ag_2O concentrations result from the applied constraints in semi-quantitative measurements by EDX. [35] Therefore, the concentration of silver at the surface should be effectively considered close to zero. In contrast, the samples subjected to the ion-exchange in KNO_3-1.0 wt% $AgNO_3$ salt are characterized by significant amounts of silver on the surface: The concentration of silver oxide is equal to the concentration of potassium oxide. Interestingly, the samples ion-exchanged for 4 hours exhibit larger amounts of silver, whereas the 24 hours samples contain more potassium.

The two-step ion-exchange effectively increases the silver concentration in the glass surface: the silver concentration increases with the duration of both the first and the second ion-exchange (Figure 3C). The glass produced by subsequent ion-exchanges for 4 hours and 10 minutes contains about 4 mol% of Ag_2O, whereas the Ag_2O concentration of the glass subjected to ion-exchanges for 24 hours and 30 min is 6 mol%, which is comparable with the samples subjected to ion-exchange for 24 hours.

Figure 4 shows potassium concentration profiles near the surface of samples produced by ion-exchange in pure KNO_3 for 4 and 24 hours. The potassium concentration is expressed in relative units between 100 and C_0, corresponding to the potassium concentration in the glass surface and at a depth of 2 mm from the surface, representing the as-received glass. The potassium concentration decreases continuously from the surface toward the glass center, which resembles a typical diffusion profile that can be fitted by a complementary error function:

$$C_k(x,t) = \left(C_S - C_0\right) erfc\left(\frac{x}{2\sqrt{\%Dt}}\right) + C_0 \qquad (1)$$

where x is the distance from the surface and t is ion-exchange time. C_s and C_0 are the potassium concentration on the surface

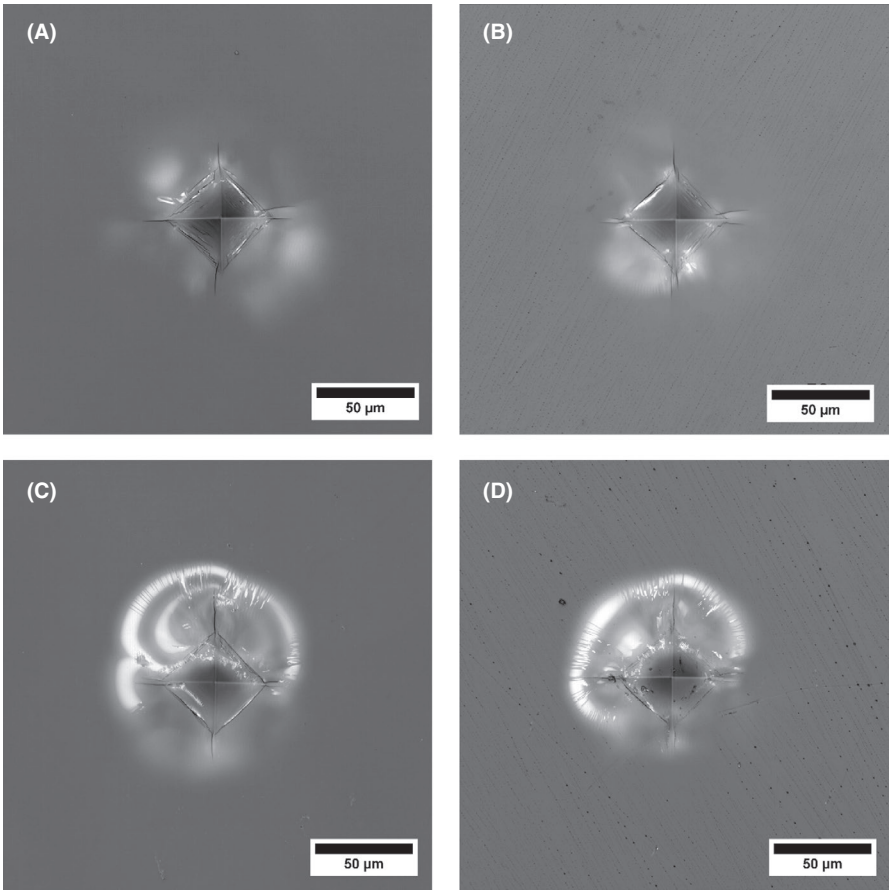

FIGURE 2 Indentations on the gas side of samples produced by two-step ion-exchange: ion-exchanged in KNO_3 for 4 h and then subjected to ion-exchange in KNO_3+ 0.2 wt% $AgNO_3$ for (A) 10 min and (B) 30 min; samples, ion-exchanged in KNO_3 for 24 h and then subjected to ion-exchange in KNO_3+ 1.0 wt% $AgNO_3$ for (C) 10 min and (D) 30 min

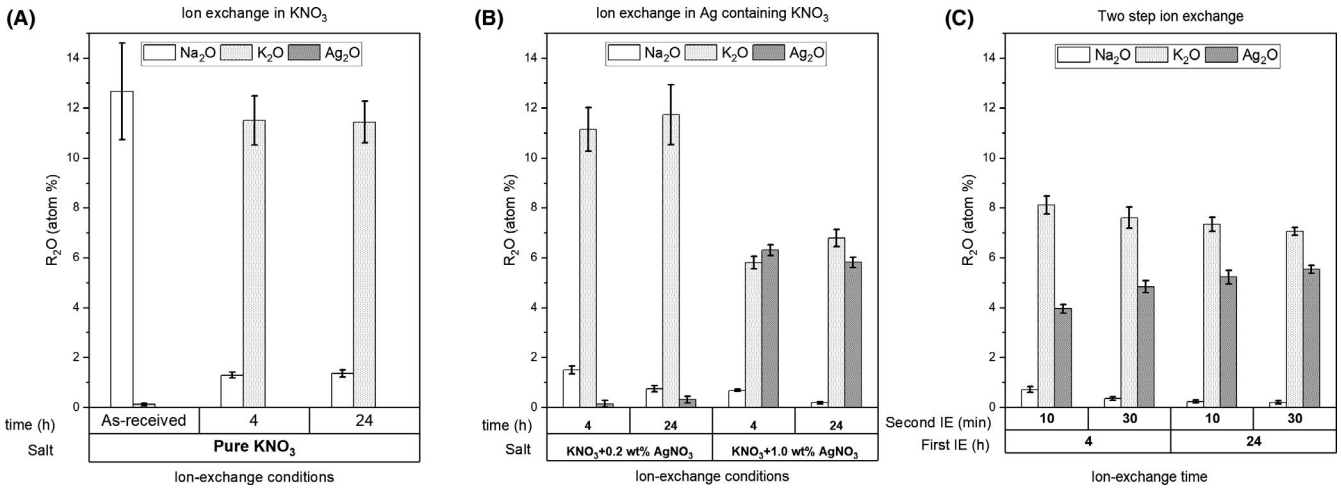

FIGURE 3 Na_2O, K_2O, and Ag_2O concentration on the glass surface before and after ion-exchange. (A) single-step ion-exchange in KNO_3, (B) single-step ion-exchange in silver-containing KNO_3, (C) two-step ion-exchange in KNO_3 and, then, KNO_3+ 1.0 wt% $AgNO_3$

and of the as-received glass, respectively. $\tilde{D}$ is the inter-diffusion coefficient, which is defined by the Nernst–Plank equation:

$$\tilde{D} = \frac{D_{Na} D_K}{D_{Na} C_{Na} + D_K C_K} \tag{2}$$

where D_i is the self-diffusion coefficient of ion i (Na^+ or K^+) and C_i is the mole fraction of the ion. Although it is reported that the interdiffusion coefficient may depend on the concentration of ions,[36-38] to simplify the estimations , $\tilde{D}$ can be considered invariable. The experimental potassium concentration profiles, Figure 4, are fitted using Eq. 1 and assuming that the inter-diffusion coefficients are constant. There is a good agreement between the experimental data and fitting curve, presented by solid lines, suggesting that the variations of inter-diffusion coefficient with concentrations are insignificant. The depth at which

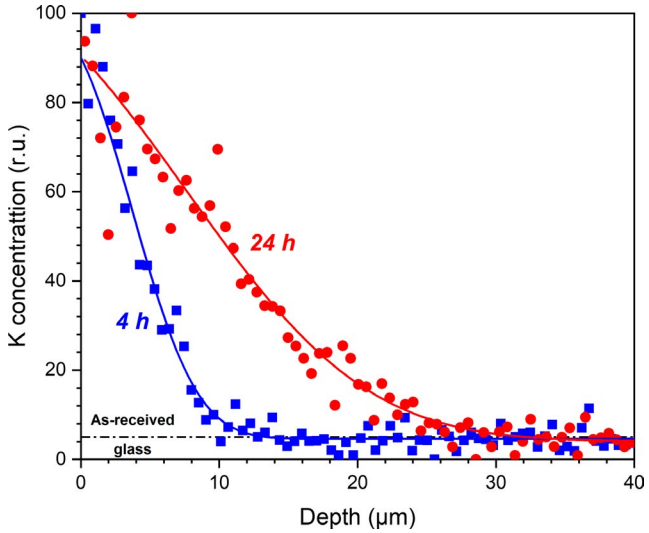

FIGURE 4 Potassium relative concentration data obtained from EDX measurements for samples ion-exchanged at 450°C in KNO_3 for 4 and 24 h; the continuous lines represent the fitting curves calculated by Eq. 1

K concentration becomes equal to the as-received glass concentration (±2%) was considered as representing the thickness of glass involved in ion-exchange, depth of layer *(DOL)*. It is 12 μm for 4 h, and 28 μm for 24 hours ion-exchange. The interdiffusion coefficients are estimated to be $1.4 \pm 0.1 \times 10^{-11}$ cm^2 s^{-1} and $1.6 \pm 0.1 \times 10^{-11}$ cm^2 s^{-1} for 4 hours and 24 hours, respectively.

Figure 5 shows potassium and silver concentration profiles produced in samples single step ion-exchanged in silver-containing salts. The potassium concentration profiles in samples produced by KNO_3+0.2 wt% $AgNO_3$ are similar to those produced in pure KNO_3. The estimated interdiffusion coefficients are $1.4 \pm 0.1 \times 10^{-11}$ cm^2 s^{-1} and $1.8 \pm 0.2 \times 10^{-11}$ cm^2 s^{-1} for 4 hours and 24 hours, respectively. These agree with the surface composition of samples indicating that the silver penetration in KNO_3+0.2 wt% $AgNO_3$ is insignificant. Conversely, in the samples ion-exchanged in KNO_3+1.0 wt% $AgNO_3$, silver-diffused deep, whereas the penetration of potassium is only slightly larger than in the samples ion-exchanged in pure KNO_3. The

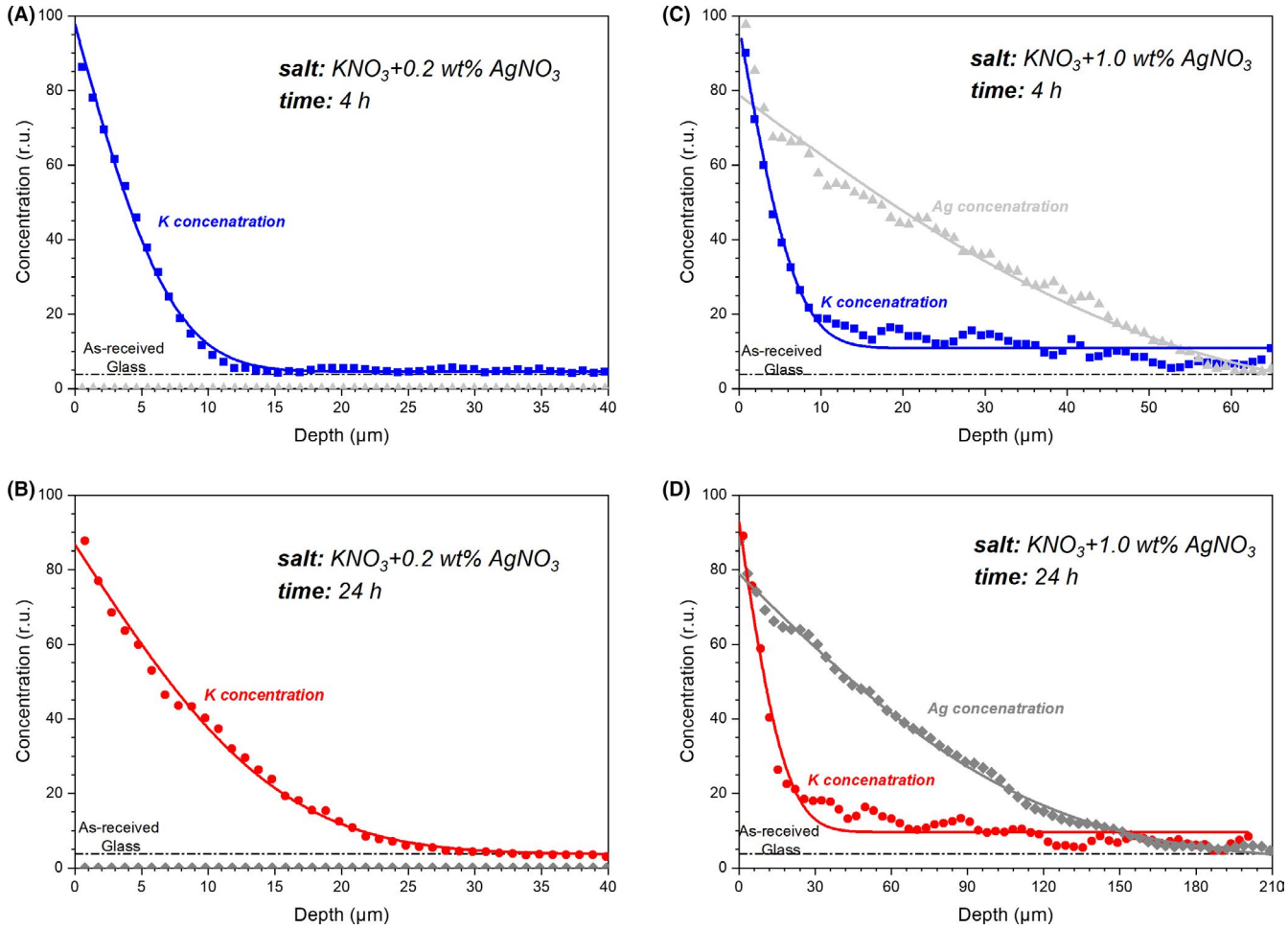

FIGURE 5 Potassium and silver relative concentration data obtained from EDX measurements for samples ion-exchanged at 450°C in KNO_3+ 0.2 wt% $AgNO_3$ for (A) 4 h and (B) 24 h, and, in KNO_3+ 1.0 wt% $AgNO_3$ for (C) 4 h and (D) 24 h. The continuous lines represent the fitting curves calculated by Eq. 1

thickness of the silver-containing layer is 60 μm after 4 hours ion-exchange and 180 μm after 24 hours, whereas the depth of the K^+-Na^+ ion-exchanged layer is 14 μm and 30 μm for 4 hours and 24 hours, respectively. There is a discrepancy between the experimental data and predicted concentration profile using Eq. 1; this is probably due to the interdependence of alkali ions and silver fluxes.[39]

Figure 6 shows potassium and silver concentration profiles in the samples subjected to two-step ion-exchange by, first, K^+-Na^+ ion-exchange in pure KNO_3 at 450°C for 4 or 24 hours, and then, immersing in KNO_3 + 1.0 wt% $AgNO_3$ salt at 400°C for 10 or 30 minutes. Two-step ion-exchange produces a silver-containing layer near the glass surface; the layer's thickness increases from 3 μm to 5 μm when the second ion-exchange duration increases from 10 to 30 minutes. The Ag^+-K^+ ion-exchange at the surface resulted in a decrease in potassium concentration, and consequently, the maximum of K concentration profiles was moved to the depth of 2-3 μm in samples initially ion-exchanged for 24 hours (Figure 6 c and d). It should be noted that the second ion-exchange has no significant influence on the depth of the Na^+-K^+ ion-exchanged layer.

Figure 7 shows the normalized silver release of ion-exchanged samples after being immersed in distilled water at 40°C for 24 hours. The concentration of released silver, Q_{Ag}, was calculated according to:

$$Q_{Ag} = \frac{(C_{Ag} - C_B) \bullet V}{S} \tag{3}$$

where C_{Ag} and C_B are the silver concentrations in the experiment solution and the reference solution, respectively. S is the surface area of the sample subjected to ion-release experiments, and V is the volume of the corrosion solution.

The variations in silver concentration in the liquid for the samples produced by ion-exchange in KNO_3 +0.2 wt% $AgNO_3$ was below the detection limit of ICP analysis and, therefore, the silver release was considered zero and is not shown in Figure 7. The silver release of samples subjected to single-step ion-exchange is about 1.0 μg.cm^{-2} and independent of the ion-exchange conditions. In contrast, the increase in second step ion-exchange time from 10 to 30 minutes decreases the silver release: from 3.0 to 2.0 μg.cm^{-2} for samples

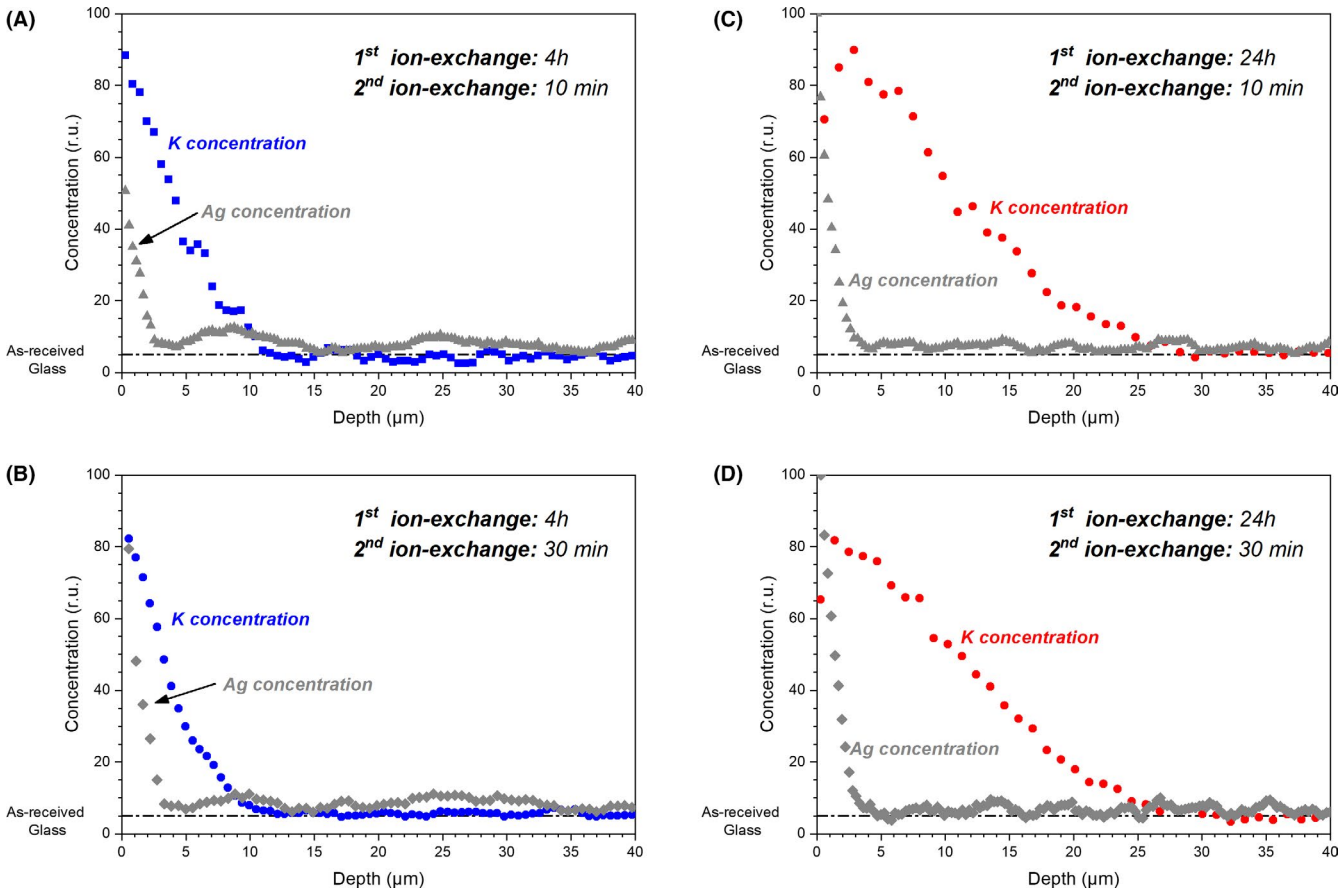

FIGURE 6 Potassium and silver relative concentration data obtained from EDX measurements for samples produced by two-step ion-exchange: first ion-exchanged in KNO_3 for 4 h, then, ion-exchanged in KNO_3+ 1.0 wt% $AgNO_3$ for (A) 10 min and (B) 30 min. and, first ion-exchanged in KNO_3 for 24 h, then, ion-exchanged in KNO_3+ 1.0 wt% $AgNO_3$ for (C) 10 min and (D) 30 min

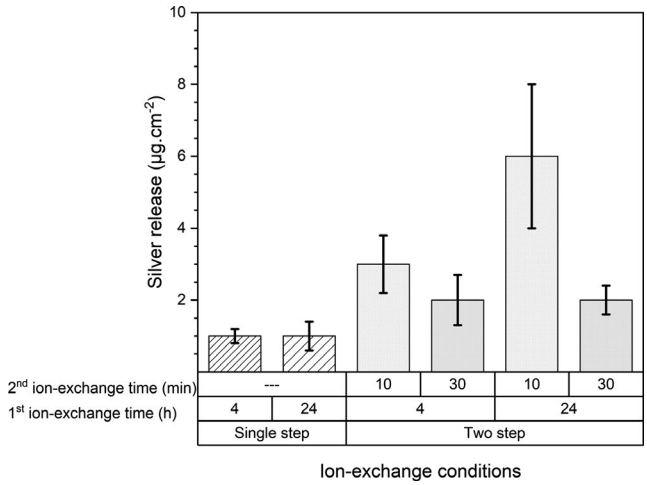

FIGURE 7 Silver release of ion-exchanged glass after 24 h immersion in DI-water after at 40°C

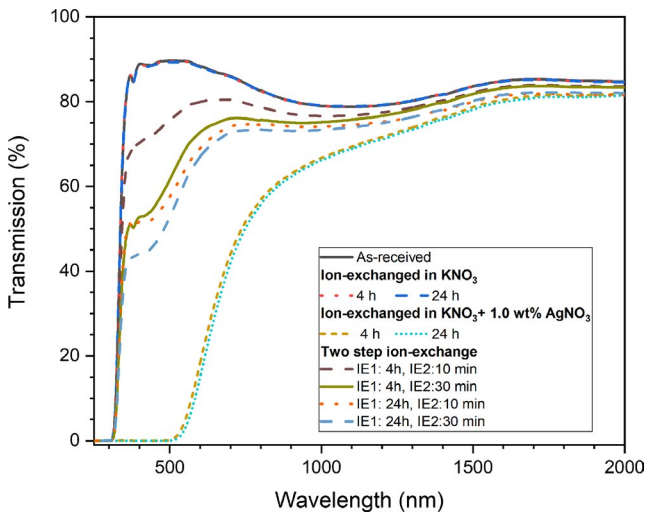

FIGURE 8 In-line transmittance against the wavelength of as-received glass and samples produced by ion-exchange

ion-exchanged for 4 hours, and from 6.0 to 2.0 µg.cm^{-2} or samples ion-exchanged for 24 hours.

The samples exposed to the silver-containing salt appeared yellowish-brown. The discoloration is observed in particular on the tin-side of the glass. Figure 8 shows the transmission spectra from ultraviolet to the near-infrared range of glasses after ion-exchange in KNO_3 + 1.0 wt% $AgNO_3$ salt. The spectra of as-received glass and Na^+-K^+ ion-exchanged samples are also shown for comparison. It should be noted the transmission spectra are unavoidably affected by light interaction with both glass surfaces; thus, the colored surface, tin side, mainly determines the optical characteristics of glass. Although the glasses subjected to pure KNO_3 exhibit a spectrum identical to the as-received glass, the transparency of samples ion-exchanged in KNO_3 + 1.0 wt% $AgNO_3$ decreased. The loss of transparency is significant in the case of single-step ion-exchange glasses. Moreover, the ultraviolet cut-off of samples subjected to single-step ion-exchange is shifted from 310 nm to 500 nm. Two-step ion-exchanged samples exhibit higher transmission than the samples produced by the single ion-exchange in silver-containing salts. In the case of two-step ion-exchange, the increase in either first or second ion-exchange time decreases the light transmission of samples.

4 | DISCUSSION

During chemical strengthening, the surface compressive stress is generated by the *stuffing* of larger potassium ions into the smaller sodium sites in the glass surface and the dilation of the glass network.[23,24] Although the compressive stress build-up during chemical strengthening is a complex process,[40] the surface compression, intuitively, depends on the size of invading ions and the produced concentration profile. Ion-exchange at 450°C for 4 hours replaces almost all sodium with potassium at the glass surface, producing compressive stress of about 550 MPa. Despite the very similar surface composition of glass after 24 hours ion exchange, the samples show smaller surface compression (about 450 MPa) due to the stress relaxation below the glass-transition temperature.[41] Silver can exist in soda-lime silicate glass in the form of individual ions, atoms, or clusters depending on its chemical state: Ag^+, Ag^0, or Ag^{2+}, respectively.[17,42] Although the EDS analysis cannot determine the chemical state of silver, the experimental results confirm that silver is present in the glass, and the semi-quantitative results can be used to compare the concentration of silver.

The equilibrium between the glass and salt bath determines the concentration of stuffed cations (i.e., K^+ and Ag^+) and, in turn, the surface compression. Araujo et al. proposed a thermodynamic model describing the equilibrium concentration of salt bath cations on the glass surface[43,44]: the surface concentration of the salt's cations is a sigmodal function of their concentration in the bath. The obtained results have indicated that the lower concentration of Ag^+ in the salt (0.2 wt% $AgNO_3$) is not sufficient to introduce a significant amount of silver to the glass surface, while using 1.0 wt% $AgNO_3$ can change the surface composition. It is interesting to point out that although the molar ratio of Ag^+/K^+ is very limited ($Ag^+/K^+ \approx 10^{-4}$), the silver concentration on the surface is significant, which is probably accounted for by the preferential Ag^+-Na^+ ion-exchange, micro-inhomogeneity of salt, and different ion mobility. However, stuffing smaller silver ions instead of larger potassium ions results in the production of smaller surface compression.

Moreover, small changes in salt composition, particularly, small monovalent ions, can accelerate the relaxations

mechanisms at the surface resulting in the decrease in residual stress[45]; this is probably responsible for the smaller surface compression in samples subjected to ion-exchange in KNO_3 + 0.2 wt% $AgNO_3$ despite the amount of potassium similar to the samples treated in pure KNO_3.

Surface compression is another factor influencing the exchange of monovalent ions in the glass.[46] Due to the low treatment temperature, 400°C, the surface compression of ion-exchanged samples remains substantially unchanged (Tables 1 and 2). Figure 9 shows the Ag_2O concentration as a function of surface compression in samples subjected to two-step ion-exchange. The samples whose surface compression is smaller show a higher silver concentration after the second ion-exchange. According to the theory of chemical strengthening, surface compression is produced at the expense of a decrease in glass *free volume* during the *stuffing* of larger potassium ions into sodium sites; thus, the glass with larger surface compression has less free volume available for K^+-Ag^+ ion-exchange.[22,47,48]

The Ag^+-Na^+ layer thickness is significantly larger than the K^+-Na^+ one in the samples subjected to ion-exchange in KNO_3+ 1.0 w% $AgNO_3$ salt. Due to their size, the higher diffusivity of Ag^+ ions is responsible for the deep penetration during the Ag^+-Na^+ ion-exchange. Moreover, the depth of the K^+-Na^+ ion-exchanged layer, *DOL*, is larger in samples in which silver concentration profiles are produced. It is interesting to compare the effect of ion-exchange time on the penetration depth of potassium into the glass. According to Eq. 1, the *DOL* is proportional to the square root of time: it is therefore expected that the *DOL* increases by the factor of ≈2.4 when the ion-exchange time increases from 4 to 24 hours. While the ratio of *DOL*s of samples ion-exchanged for 24 hours and 4 hours in pure KNO_3 and KNO_3+ 0.2 w% $AgNO_3$ is about ≈2.3, it is ≈3.1 for samples treated in KNO_3+ 1.0 w% $AgNO_3$. A more complex model is required to calculate ion-exchanged depth when the fluxes of diffusing elements (Na^+, K^+, and Ag^+) are influenced by each other.[39] Nevertheless, the diffusion of monovalent cations can be described using a conservative explanation. Ag^+, owing to its high diffusivity, penetrates faster than potassium ions. Therefore, the ion-exchange process can be considered to consist of two events: first, Ag^+-Na^+ exchanged at the frontier of ion-exchanged layers and, then, Ag^+-Na^+ and K^+-Na^+ exchange close to the glass surface. It is reported that Ag^+-Na^+ ion-exchange changes the cation environment and coordination number and, thus, the glass structure[49,50]; this might facilitate further diffusion of potassium ions into the glass. However, more studies are required to understand how ion-exchange influences further diffusion of ions.

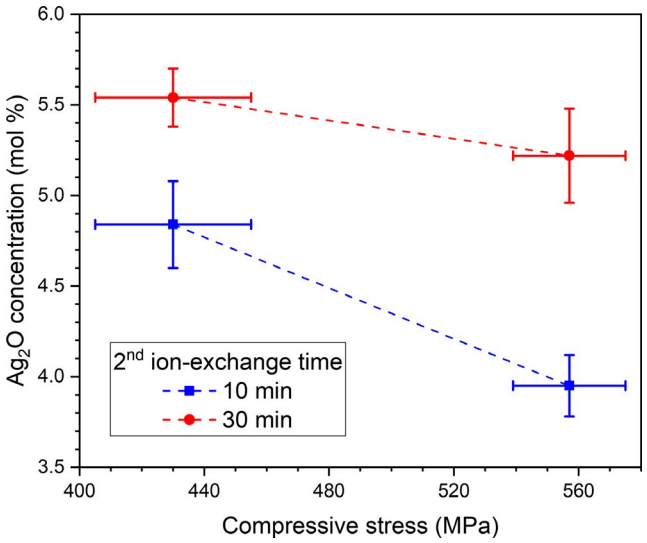

FIGURE 9 Ag_2O concentration on the surface of glass subjected to two-step ion-exchange against compressive stress produced in the first step (dashed lines are to guide the eyes)

The produced K^+-Na^+ ion-exchanged layers generate compressive stress of sufficient depth to reinforce the surface flaws formed during the glass processing and increase the glass strength.[51] Although the single ion-exchange in KNO_3+ 1.0 w% $AgNO_3$ produced limited compressive stress on the glass's surface, the second ion-exchange has no detrimental effect on the surface compression. Therefore, the two-step ion-exchange can be potentially used as a practical approach to introduce silver to the glass surface.

Based on the obtained ion-release results, two-step ion-exchanged samples are capable of releasing silver ions, which enables the anti-bacterial activity of glass surfaces. Indeed, chemical strengthening parameters influence the silver concentration in the glass surface, the silver release, and, in turn, the anti-bacterial properties. It is known that the residual compressive stress decreases the mobility of alkali ions in glass and, therefore, has a negative influence on the release of silver.[46] However, whether Na^+-K^+ ion-exchange can be exploited to modify the release of silver ions is questionable. Figure 10 shows the silver release of samples produced by two-step ion-exchange as a function of surface Ag_2O concentration; the results for the glass prepared by single-step ion exchange are also shown for comparison. Although single-step ion-exchange produced the highest Ag_2O concentration, silver release is lowest; moreover, the samples subjected to the second ion-exchange for 30 minutes exhibit smaller silver release despite their higher Ag_2O concentration. One might speculate that the surface compression is the only parameter that has an evident influence on the silver release; however, the similar silver release after the second ion-exchange for 30 minutes from samples produced using different initial steps indicates that other parameters may also be at play. The glass surface structure is another factor playing an influential role in the silver release. Although

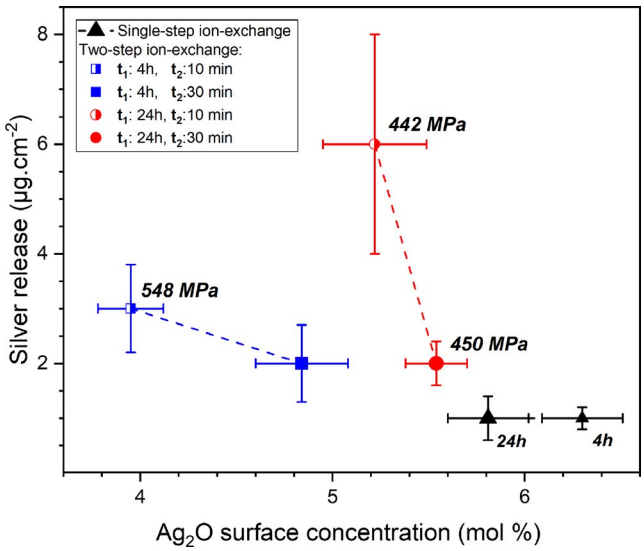

FIGURE 10 Silver release vs Ag_2O concentration on the surface of glass subjected to ion-exchange (dashed lines are to guide the eyes)

it is well-known that the glass structure undergoes a series of structural changes by stuffing larger ions during chemical strengthening,[52] how exchanging larger cations with smaller ions changes the glass structure is still equivocal. Moreover, the establishment of the thermal equilibrium between the salt bath and the glass surface may take some time. Apparently, 30 minutes ion-exchange provides enough time for establishing new equilibrium conditions between the salt bath and glass surface, and, consequently, the samples show similar silver-release behavior regardless of the first step ion-exchange or surface compressive stress. Nevertheless, further studies are needed to understand how the second step ion-exchange can influence the surface properties of glass and the silver release kinetics.

5 | CONCLUSIONS

Two-step ion-exchange was successfully employed in order to produce silver releasing surfaces in glasses subjected to chemical strengthening without impairing the surface compressive stress: These glasses are simultaneously strengthened and silver-releasing. Applying different times of ion-exchange on a commercial soda-lime silicate float glass produces different surface compression and depth of modified layer, resulting in different silver release behavior that can be correlated to different extents of surface compression.

Although the silver release was limited in the glass with larger surface compression, other parameters, such as the second step ion-exchange duration, seem to be influential in silver release. Careful design of the duration of the second ion-exchange step appears to be the key to efficient tailoring of release behavior. It will be necessary to verify the impacts of other parameters such as temperature and the salt bath composition on the efficiency of ion-exchange and, thus, silver release.

ACKNOWLEDGMENTS

This paper is a part of the dissemination activities of the project FunGlass. This project has received funding from the European Union's Horizon 2020 research and innovation program under grant agreement No 739566. The financial support of this work by the grants VEGA 1/0191/20 and 2/0028/21 is gratefully acknowledged. The authors appreciate the help of Dr. R Klement with measuring optical properties and AGC Trenčín, s.r.o. for the donation of float glass used in this study.

ORCID

Ali Talimian https://orcid.org/0000-0002-4076-2160
Hana Kaňková https://orcid.org/0000-0001-5494-9754
Dagmar Galusková https://orcid.org/0000-0003-4114-1048
Lothar Wondraczek https://orcid.org/0000-0002-0747-3076
Dusan Galusek https://orcid.org/0000-0001-5995-8780

REFERENCES

1. Esteban-Tejeda L, Malpartida F, Esteban-Cubillo A, Pecharromán C, Moya JS. The antibacterial and antifungal activity of a soda-lime glass containing silver nanoparticles. Nanotechnology. 2009;20(8):085103.
2. Kosik Williams C, Borrelli NF, Senaratne W, Wei Y, Petzold O. Touchscreen surface warfare-Physics and chemistry of antimicrobial behavior of ion-exchanged silver in glass. Am Ceram Soc Bull. 2014;93(4):20–4.
3. Adlhart C, Verran J, Azevedo NF, Olmez H, Keinänen-Toivola MM, Gouveia I, et al. Surface modifications for antimicrobial effects in the healthcare setting: a critical overview. J Hosp Infect. 2018;99(3):239–49.
4. Page K, Wilson M, Parkin IP. Antimicrobial surfaces and their potential in reducing the role of the inanimate environment in the incidence of hospital-acquired infections. J Mater Chem. 2009;19(23):3819–31.
5. Crijns FRL, Keinänen-Toivola MM, Dunne CP. Antimicrobial coating innovations to prevent healthcare-associated infection. J Hosp Infect. 2017;95(3):243–4.
6. Zada T, Reches M, Mandler D. Antifouling and antimicrobial coatings based on sol–gel films. J Sol-Gel Sci Technol. 2020;95(3):609–19.
7. Estekhraji SAZ, Amiri S. Sol–gel preparation and characterization of antibacterial and self-cleaning hybrid nanocomposite coatings. J Coat Technol Res. 2017;14(6):1335–43.
8. Riaz M, Zia R, Saleemi F, Hussain T, Bashir F, Ikhram H. Effect of Ti+4 on in vitro bioactivity and antibacterial activity of silicate glass-ceramics. Mater Sci Eng, C. 2016;69:1058–67.
9. Gross TM, Lahiri J, Golas A, Luo J, Verrier F, Kurzejewski JL, et al. Copper-containing glass ceramic with high antimicrobial efficacy. Nat Commun. 2019;10(1):1979.
10. Demirel B, Erol Taygun M. Production of soda lime glass having antibacterial property for industrial applications. Materials. 2020;13(21):4827.

11. Nielsen KH, Wondraczek K, Schubert US, Wondraczek L. Large-area wet-chemical deposition of nanoporous tungstic silica coatings. J Mater Chem C. 2015;3(38):10031–9.
12. Thurman RB, Gerba CP, Bitton G. The molecular mechanisms of copper and silver ion disinfection of bacteria and viruses. Crit Rev Environ Control. 1989;18(4):295–315.
13. Borrelli NF, Morse DL, Senaratne W, Verrier F, Wei Y. Coated, antimicrobial, chemically strengthened glass and method of making. United States US8753744B2. 2014.
14. Huang W-L. Method of fabricating an anti-glare, strengthened, anti-microbial and antifingerprint strengthened glass. United States US20180141854A1. 2018.
15. Manikandan D, Mohan S, Magudapathy P, Nair KGM. Blue shift of plasmon resonance in Cu and Ag ion-exchanged and annealed soda-lime glass: an optical absorption study. Physica B. 2003;325:86–91.
16. Karlsson S, Wondraczek L, Ali S, Jonson B. Trends in effective diffusion coefficients for ion-exchange strengthening of soda-lime-silicate glasses. Front Mater. 2017;4: https://doi.org/10.3389/fmats.2017.00013.
17. Borsella E, Battaglin G, Garcìa MA, Gonella F, Mazzoldi P, Polloni R, et al. Structural incorporation of silver in soda-lime glass by the ion-exchange process: a photoluminescence spectroscopy study. Appl Phys A. 2000;71(2):125–32.
18. Dubiel M, Brunsch S, Kolb U, Gutwerk D, Bertagnolli H. Experimental studies investigating the structure of soda-lime glasses after silver-sodium ion exchange. J Non-Cryst Solids. 1997;220(1):30–44.
19. Quaranta A, Cattaruzza E, Gonella F. Modelling the ion exchange process in glass: phenomenological approaches and perspectives. Mater Sci Eng, B. 2008;149(2):133–9.
20. Honkanen S, West BR, Yliniemi S, Madasamy P, Morrel M, Auxier J, et al. Recent advances in ion exchanged glass waveguides and devices. Phys Chem Glasses: Eur J Glass Sci Technol B. 2006;47(2):110–20.
21. Karlsson S, Jonson B, Stålhandske C. The technology of chemical glass strengthening – a review. Glass Technol: Eur J Glass Sci Technol A. 2010;51(2):41–54.
22. Varshneya AK. The physics of chemical strengthening of glass: room for a new view. J Non-Cryst Solids. 2010;356(44):2289–94.
23. Varshneya AK. Chemical strengthening of glass: lessons learned and yet to be learned. Int J Appl Class Sci. 2010;1(2):131–42.
24. Gy R. Ion exchange for glass strengthening. Mater Sci Eng, B. 2008;149(2):159–65.
25. Gross TM. Chemical Strengthening of Glass. In: Musgraves JD, Hu J, Calvez L, editors. Springer Handbook of Glass. Cham: Springer International Publishing; 2019:273–96.
26. Guldiren D, Aydın S. Antimicrobial property of silver, silver-zinc and silver-copper incorporated soda lime glass prepared by ion exchange. Mater Sci Eng, C. 2017;78:826–32.
27. Guldiren D, Erdem İ, Aydin S. Influence of silver and potassium ion exchange on physical and mechanical properties of soda lime glass. J Non-Cryst Solids. 2016;441:1–9.
28. Abrams MB, Green DJ, Jill GS. Fracture behavior of engineered stress profile soda lime silicate glass. J Non-Cryst Solids. 2003;321(1):10–9.
29. Sglavo VM, Prezzi A, Zandonella T. Engineered stress-profile silicate glass: high strength material insensitive to surface defects and fatigue. Adv Eng Mater. 2004;6(5):344–9. http://dx.doi.org/10.1002/adem.200300509.
30. ASTM Standard. C338-93. In: Test Method for Softening Point of Glass. ASTM Book of Standards. West Conshohocken, PA: ASTM International; 2019. http://www.astm.org/cgi-bin/resolver.cgi?C338-93(2019). Accessed January 20, 2021.
31. ASTM Standard. C1279-13. In: Test Method for Non-Destructive Photoelastic Measurement of Edge and Surface Stresses in Annealed, Heat-Strengthened, and Fully Tempered Flat Glass. ASTM Book of Standards. West Conshohocken, PA: ASTM International; 2019. http://www.astm.org/cgi-bin/resol ver.cgi?C1279 -13(2019). Accessed January 20, 2021.
32. Atılgan S, Özben N, Sökmen İ, Wondraczek L, Akman S. Effect of surface cleaning prior to chemical strengthening process of glass. Int J Appl Glass Sci. 2020;11(4):720–9.
33. Sglavo VM, Talimian A, Ocsko N. Influence of salt bath calcium contamination on soda lime silicate glass chemical strengthening. J Non-Cryst Solids. 2017;458:121–8.
34. Aben H, Guillemet C. Determination of the Total Stresses. In: Aben H, Guillemet C, editors. Photoelasticity of Glass. Berlin, Heidelberg: Springer; 1993:139–61.
35. Wernisch J, Röhrbacher K. Standardless Analysis. In: Love G, Nicholson WAP, Armigliato A, editors. Modern Developments and Applications in Microbeam Analysis. Vienna: Springer; 1998:307–16.
36. Shen J, Green DJ, Pantano CG. Control of concentration profiles in two step ion exchanged glasses. Phys Chem Glasses. 2003;44(4):284–92.
37. Jiang L, Guo X, Li X, Li L, Zhang G, Yan Y. Different K+–Na+ inter-diffusion kinetics between the air side and tin side of an ion-exchanged float aluminosilicate glass. Appl Surf Sci. 2013;265:889–94.
38. Varshneya AK, Milberg ME. Ion exchange in sodium borosilicate glasses. J Am Ceram Soc. 1974;57(4):165–9.
39. Slyusarenko EM, Soldatov VS. Description of interdiffusion processes in multicomponent systems by the first Fick's law. Phys Status Solidi B Basic Solid State Phys. 1989;154(2):475–82. http://dx.doi.org/10.1002/pssb.2221540207.
40. Varshneya AK, Olson GA, Kreski PK, Gupta PK. Buildup and relaxation of stress in chemically strengthened glass. J Non-Cryst Solids. 2015;427:91–7.
41. Shen J, Green DJ, Tressler RE, Shelleman DL. Stress relaxation of a soda lime silicate glass below the glass transition temperature. J Non-Cryst Solids. 2003;324(3):277–88.
42. Zhang AY, Suetsugu T, Kadono K. Incorporation of silver into soda-lime silicate glass by a classical staining process. J Non-Cryst Solids. 2007;353(1):44–50.
43. Araujo R. Thermodynamics of ion exchange. J Non-Cryst Solids. 2004;349:230–3.
44. Araujo RJ, Likitvanichkul S, Thibault Y, Allan DC. Ion exchange equilibria between glass and molten salts. J Non-Cryst Solids. 2003;318(3):262–7.
45. Seaman JH, Lezzi PJ, Blanchet TA, Tomozawa M. Degradation of ion-exchange strengthened glasses due to surface stress relaxation. J Non-Cryst Solids. 2014;403:113–23.
46. Varshneya AK, Dumais GA. Influence of externally applied stresses on kinetics of ion exchange in glass. J Am Ceram Soc. 1985;68(7):C-165–C-166.
47. Kreski PK, Varshneya AK, Cormack AN. Investigation of ion-exchange "stuffed" glass structures by molecular dynamics simulation. J Non-Cryst Solids. 2012;358(24):3539–45.
48. Ingram MD. Towards a theory of ion transport in glass. Physica A. 1999;266(1):390–9.

49. Yano T, Nagano T, Lee J, Shibata S, Yamane M. Cation site occupation by Ag+/Na+ ion-exchange in R_2O–Al_2O_3–SiO_2 glasses. J Non-Cryst Solids. 2000;270(1):163–71.
50. Catan F, De Sousa Meneses D, Blondeau JP, Allam L. Structural changes of Ag+–Na+ ion exchanged soda-lime glasses investigated by scanning electron microscopy and infrared reflectivity. J Non-Cryst Solids. 2008;354(10):1026–31.
51. Bradt RC. The fractography and crack patterns of broken glass. J Fail Anal and Preven. 2011;11(2):79–96.
52. Ingram MD, Wu M-H, Coats A, Kamitsos EI, Varsamis CP, Garcia N, et al. Evidence from infrared spectroscopy of structural relaxation during field assisted and chemically driven ion exchange in soda–lime–silica glasses. Phys Chem Glasses. 2005;46(2):84–9.

How to cite this article: Talimian A, Nowicka A, Kaňková H, et al. Two-step ion-exchanged soda lime silicate glass: Effect of surface compression on silver ion release. *Int J Appl Glass Sci*. 2021;00:1–12. https://doi.org/10.1111/ijag.15919